More radial trace domain applications

David C. Henley

ABSTRACT

The radial trace domain, less well-known than other transform domains, has been shown to be a particularly effective one for attenuating source-generated coherent noise on seismic data. In a closely related application, the radial domain can be used for selectively enhancing specific components of seismic wavefields. Use can also be made of the intrinsic interpolation in the transform algorithm itself to uniformly re-map seismic trace gathers with irregular trace spacing, or to map the data to diagnostic domains such as the X^2-T^2 domain. In yet another application, the origin of the radial domain can be used as a centre around which to rotate sea-floor reflections and their simple multiples from a sloping to a horizontal sea-floor to enhance multiple removal. Finally, a hybrid radial trace transform has been implemented to generate traces for which raypaths follow Snell's law for use in AVA (Amplitude versus Angle) studies. Shown here are examples of all the above applications.

INTRODUCTION

The radial trace transform was introduced by the Stanford Exploration Project many years ago (Ottolini, 1979), (Claerbout, 1983), primarily for use in migration and imaging applications. It has been shown subsequently, because of its particular geometry, to be very useful for wavefield separation (Claerbout, 1983) and coherent noise attenuation (Henley, 1999). The radial trace transform, unlike such transforms as the F-K transform, is a mapping transform which takes each point of the X-T plane into a point of the R-T plane, and vice versa for the inverse. Since the transform is an interpolator, not an integrator, there is no restriction on the portion of the original domain to be mapped. Also, there are not any inherent restrictions on the interpolation method (Henley, 1999), so that interpolation may be chosen to suit the particular application.

Earlier work focused primarily on the noise attenuation application in the radial trace domain, but suggested that wavefield separation in general could also be done in the radial domain (Henley, 1999). This particular application is shown here with an example from a 3-C walk-away VSP, which, because of its relatively small number of receiver levels (10) and its relatively low signal-to-noise ratio, proves to be a challenge to more traditional wavefield separation methods.

One of the important advantages of the radial transform with respect to better known transforms such as the F-K transform is the ability to transform non-uniformly sampled data, such as a shot gather with irregular source-receiver offset values. The receiver-line gathers of a 3-D shot are a prime example. This ability is due principally to the choice of interpolation routine in the transform itself, often a two-point method in the interest of speed and data fidelity. Since the inverse transform is also a point-to-

point mapping with intrinsic interpolation, virtually any set of co-ordinate grid points can be substituted for the ones from the original input gather, to be used for the reconstituted X-T gather, as long as all of the new co-ordinate values fall within the range of those on the original gather. To demonstrate this feature, a model shot gather originally uniformly sampled in both offset and travel time is transformed to the R-T domain, then back to the X-T, X^2-T, or X^2-T^2 domains, which are only a few of the possibilities.

The simple radial trace transform maps input seismic data into traces of constant apparent velocity. This means that for a constant-velocity medium, like the ocean, reflections from planar boundaries like the idealised sea-floor can be rotated in the 2-D plane simply by adding a constant to the velocity co-ordinates of the radial traces before the inverse R-T transform and applying linear moveout in the X-T domain after the inverse. Hence, a sea-floor reflection from a sloping sea-floor can be rotated in the R-T domain to its equivalent flat lying position. The surface multiples from this reflection can also be rotated to their flat lying equivalent positions, but for each order of multiple, the rotation increases by an additional amount equivalent to the sea-floor slope. One way to capture the reflection and its multiples and approximately rotate them in one operation is to use non-linear radial traces that are arcs of circles, the curvature determined by the velocity of the uniform velocity layer (water) and the slope of the sea-floor. This is demonstrated using synthetic shot gathers.

While simple radial traces simulate seismic data recorded along straight raypaths for a constant velocity medium, a modified R-T transform can generate "Snell ray traces", which capture seismic energy travelling along raypaths obeying Snell's Law. This is accomplished by computing the local "refractive index" as a function of travel time from an input velocity function and using the refractive index to control the divergence/convergence of the fan of radial traces as a function of travel time. A familiar shot gather is used to demonstrate this mode of radial trace transform.

WAVEFIELD SEPARATION

To illustrate the wavefield separation application in the radial trace domain, a 3-C walk-away VSP survey from the Blackfoot prospect (Xu et al, 1999), was selected. Because there are only ten levels recorded for each of thirty shots, wavefield separation based on the coherence of events across single shot gathers is less effective than would be the case for a single offset VSP with many levels recorded in the borehole. To deal with this problem, a supergather was formed from all the traces in the survey, sorted by source-borehole offset, then by receiver elevation. When arranged in this fashion, as in Figure 1, various coherent events in the supergather can be approximately aligned by application of NMO to correct approximately for source-borehole offset, followed by linear moveout to correct for receiver elevation difference. The linear moveout can be selected to align either the downgoing or the upcoming wavefronts, depending upon which events are desired to be enhanced. Note that it is not necessary to use exact NMO or linear moveout for the alignment, since the aim is to align coherent events only well enough to attenuate or enhance them using the radial trace dip filter. Figure 2 shows the supergather from Figure 1, after

NMO and linear moveout correction to align the upcoming wavefield events horizontally. A number of linear wavefield events are aligned across several individual common offset gathers by this process, thus increasing their coherence length. To assist in the separation process, the source-receiver offset trace headers are temporarily replaced with artificially generated pseudo-offsets to give the supergather the attributes of a source gather. To isolate the horizontally oriented upcoming wavefield, each of the separate dipping linear wavefield components is attenuated in succession, starting with the strongest or most obvious. The attenuation is accomplished by measuring the apparent velocity of a linear component and applying a radial trace dip filter (Henley, 1999), using either the low-cut filter option, or the low-pass and subtract option. Often, a linear component having a particular apparent velocity is accompanied by a component of the same velocity, but opposite dip, which must be removed using a radial dip filter with the negative of the original velocity. After removal of all obvious dipping linear components, the remanent wavefield can be moved out with a linear velocity, enhanced with a radial dip filter in the low-pass mode, and the linear velocity removed. This further reduces residual dipping wavefield components and attenuates random noise. The result of the separation process is shown in Figure 3 for the vertical component of the upcoming wavefield. This supergather can now have its original headers restored and the linear and hyperbolic moveout restored; the supergather can then be separated into its original gathers for further VSP processing as desired.

A more challenging prospect is presented by the inline component of this same Blackfoot data set, because the signal-to-noise ratio is much smaller. The same procedure can be used, however, to extract the upcoming inline wavefield. Figure 4 shows the inline component as a supergather while Figure 5 displays the supergather with appropriate NMO and linear moveout corrections. Figure 6 shows the result of the completed separation. The greater strength of the events away from the centre of the supergather (the borehole position) confirms that they are likely upcoming P-S converted waves, the desired outcome. As before, this supergather can be subsequently restored to individual gathers for further conventional VSP processing.

INTERPOLATION AND GRIDDING

Since interpolation is an essential part of the radial trace transform and its inverse (Henley, 1999), it is quite easy to use the transform pair to alter the sample grid points of the input ensemble in the X-dimension. For an input gather with irregularly spaced traces, the data can be regridded to uniform spacing as long as the new offsets lie within the range of the old values. Data which are too sparsely sampled in the X-dimension, and hence exhibit aliasing on some events, can in some cases be interpolated to a finer trace spacing, thus reducing the aliasing. Finally, certain non-linear offset distributions may be useful for diagnostics (for example, an X^2 distribution). The simple two-point interpolation scheme used in the current CREWES radial trace algorithms lends itself readily to these re-gridding applications, as shown in the following examples.

The synthetic marine shot gather shown in Figure 7 was generated by Brian Hoffe of CREWES for use in studying OBC data. It is so sparsely sampled in the offset dimension that several events, particularly those that are water-borne, are badly aliased. This limits processing options for such purposes as water multiple removal to those that are single-trace operations. The same synthetic shot gather is featured in Figure 8 after having its offset increment decreased from 50 m to 5 m using the radial trace transform and its inverse. In order to diminish the aliasing of the water-borne energy while at the same time not introducing aliasing into the faster events beneath, a partial NMO correction was applied to the gather before the radial trace transform and inverse, and removed later. Clearly, in Figure 8, the water-borne energy is no longer aliased and is now appropriate for the application of multi-trace attenuation or modelling techniques.

For diagnostic purposes, it may be desirable to map X-T space into X^2-T or even X^2-T^2, where hyperbolae are linear. Both of these mappings are available as options in the CREWES radial trace transform algorithm as illustrated in Figures 9 and 10. Furthermore, both of these mappings can also be inverted to X-T using the R-T transform.

SEA-FLOOR ROTATION

The problem of removing strong water-borne multiples from marine seismic data remains one of the more persistent problems of seismic processing. An early application for the radial trace transform was, in fact, to estimate and remove these multiples on radial traces. The radial transform restores the periodicity, amplitude, and raypath relationships of multiple and primary that exist only for near offset traces on X-T gathers (Taner, 1980). While the R-T transform domain does, in fact, restore the geometry, it does so properly only for a sea floor parallel to the sea surface. Applying R-T domain multiple attenuation over a dipping sea floor has been addressed (Lamont et al, 1999) by applying dip-corrected NMO removal to reflections and multiples from dipping interfaces. There are alternate approaches, however, which may avoid the wavelet distortion introduced by NMO correction. One such approach is to use the intrinsic geometry of the R-T transform to re-map the sloping sea-floor and its multiples onto a flat sea-floor domain. A simple primary reflection may be rotated to horizontal by adding a constant velocity value, determined as the complement of the apparent velocity (slope) of the sea-floor, to the velocity co-ordinate of each R-T trace. The inverse R-T transform will map the sample points into new X co-ordinate positions as rotated by the incremented velocity. A linear moveout correction in the X-T domain, using the apparent sea-floor velocity, is required to complete the event rotation by remapping the T co-ordinates.

A multiple reflection, however, is more complicated because its raypaths have been physically rotated by the sea-floor slope once for each bounce. From geometric optics, it can be shown that the apexes of primary and multiple hyperbolae lie on a circular arc in the X-T domain, suggesting the use of a modified R-T transform whose trace trajectories are circular arcs, the curvature determined by the sea-floor slope. Such a transform should then map corresponding points from primary and multiples

onto common radial traces. Incrementing the radial trace velocity headers by a constant and using a straight trajectory R-T inverse, followed by linear moveout in the X-T domain will approximately complete the event rotation for primary and multiples. Note that this geometric manipulation is appropriate only for a constant velocity medium, a planar interface, and simple multiples. The intent of this manipulation, then, is to rotate the sea-floor reflection and its multiples, regardless of other events, apply predictive deconvolution in the R-T domain to attenuate multiples, then reverse the rotation to restore the shot gather to its natural geometry for further conventional processing. Figure 11 shows a true-amplitude ray-traced model of two marine shot gathers generated by Pat Daley of CREWES for a sea-floor with a 7.5 degree slope. After R-T domain rotation, the gathers appear as in Figure 12. To show the processing advantage gained for multiple elimination, the autocorrelations of the R-T traces for one of the gathers in Figure 11 and its corresponding rotated version in Figure 12 are shown in Figures 13 and 14, respectively. In Figure 14, the first autocorrelation lag is nearly constant over a much larger range of R-T traces, indicating removal of much of the mis-timing introduced by the sloping sea-floor. Furthermore, the autocorrelation event peak at about 2.0 sec. corresponding to the first sub-sea-floor reflection has a nearly constant lag in Figure 13, but slopes rapidly in Figure 14. This means that this reflection is less vulnerable to inadvertent attenuation by a fixed-gap predictive operator in the rotated R-T domain than in the original R-T space.

At this time, no relation between required circular R-T trace curvature and sea-floor slope has been derived. The curvature determination is currently a trial-and-error procedure: trace curvature is varied until apexes of primary and multiples are vertically aligned in the rotated domain. Sea-floor rotation remains the subject of further experimentation and research.

SNELL RAY TRANSFORM

One of the early R-T applications described by the Stanford Exploration Project was the Snell Ray transform, in which the radial trace trajectories were not linear, but followed, instead, the paths that would be traced by rays obeying Snell's law at all interfaces. The early applications for such radial traces was in imaging and velocity diagnosis (Ottolini, 1987), but other applications can be envisioned, such as AVA (Amplitude versus Angle) diagnostics. Shot gathers transformed into Snell ray transform panels can be sorted by common velocity (takeoff angle) and used as diagnostic panels for lateral changes in subsurface lithology or fluid content. To enable this diagnostic as well as to add more versatility to the CREWES radial trace transform, the capability to generate Snell ray traces was added. The option is now available to use a velocity function to create a refractive index vector embodying Snell's Law. This vector is then used to steer each radial trace trajectory. To illustrate this new feature, Figure 15 shows a straight-ray R-T transform of a typical shot gather from the Blackfoot survey, while Figure 16 shows a Snell ray transform created from the same gather using the smoothed interval velocities from a nominal stacking velocity function for the line.

CONCLUSIONS

This report is intended as a follow-up to the introduction in 1999 of techniques for attenuation of coherent noise in the radial trace domain. Other processing applications for the radial trace transform and its inverse have been suggested and demonstrated. While some of these, like sea-floor rotation, are still under development, others, like wavefield separation and data re-gridding are in current use in projects at CREWES. In all likelihood, other useful operations involving the radial trace domain will emerge as it becomes more familiar to processors.

ACKNOWLEDGEMENTS

REFERENCES

Claerbout, J.F., 1983, Ground Roll and Radial Traces, Stanford Exploration Project Report, SEP-35, pp 43-53.

Henley, D.C., 1999, Coherent noise attenuation in the radial trace domain: introduction and demonstration, CREWES Research report **11**, pp 455-491.

Lamont, M.G., Hartley, B.M., and Uren, N.F., 1999, Multiple attenuation using the MMO and ISR preconditioning transforms: The Leading Edge, **18**, no. 1, pp 110-114.

Ottolini, R., 1979, Migration of Radial Trace Sections, Stanford Exploration Project Report, SEP-20, pp 97-115.

Ottolini, R., 1987, Data driven extraction of Snell traces, Stanford Exploration Project Report, SEP-51, pp 351-362.

Taner, M.T., 1980, Long-period sea-floor multiples and their suppression: Geophys. Prosp., **28**, no. 1, pp 30-48.

Xu, C., and Stewart, R.R., 1999, Preliminary processing and analysis of the Blackfoot walkaway VSP, CREWES Research report **11**, pp 333-344.

FIGURES

-1500 m   **Source offset**   **0**   **1500 m**
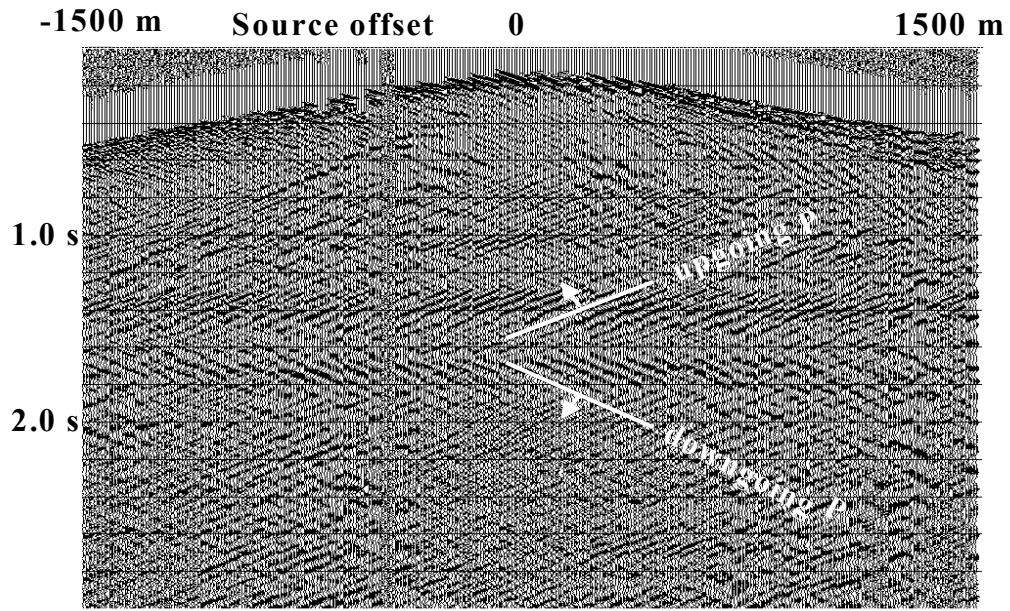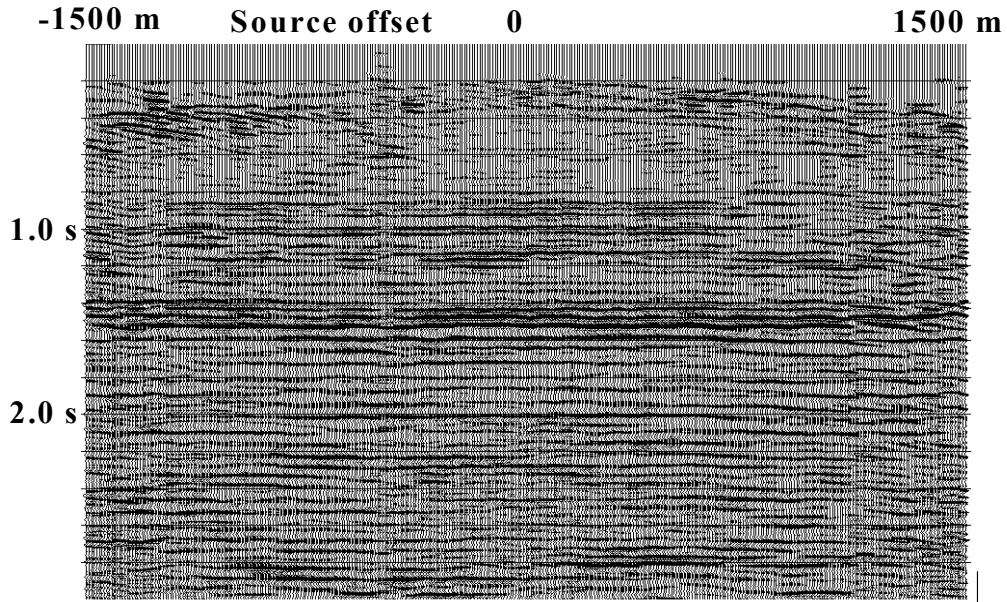

Blackfoot vsp supergather (raw vertical component wavefield)

Figure 1. Supergather formed from Blackfoot 3-C walk-away VSP vertical component data sorted by source-borehole offset and receiver level (depth in borehole). The coherence directions for upgoing and downgoing wavefronts are indicated.

-1500 m   **Source offset**   **0**   **1500 m**
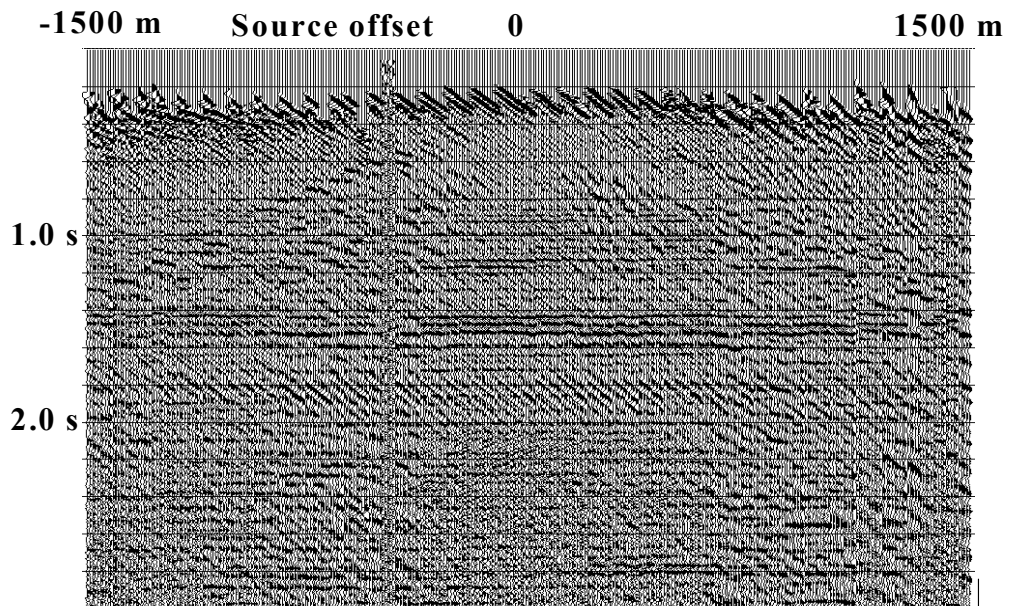
Blackfoot vsp supergather (vertical component wavefield)

Figure 2. Vertical component supergather after application of NMO for source-borehole offset and linear moveout for receiver depth.

-1500 m   **Source offset**   **0**   **1500 m**

Blackfoot vsp supergather (upgoing wavefield only)

Figure 3. Vertical supergather after several passes of radial trace dip filtering to remove unwanted wavefield components and enhance the upgoing wavefield component.

**-1500 m**   **Source offset**   **0**   **1500 m**
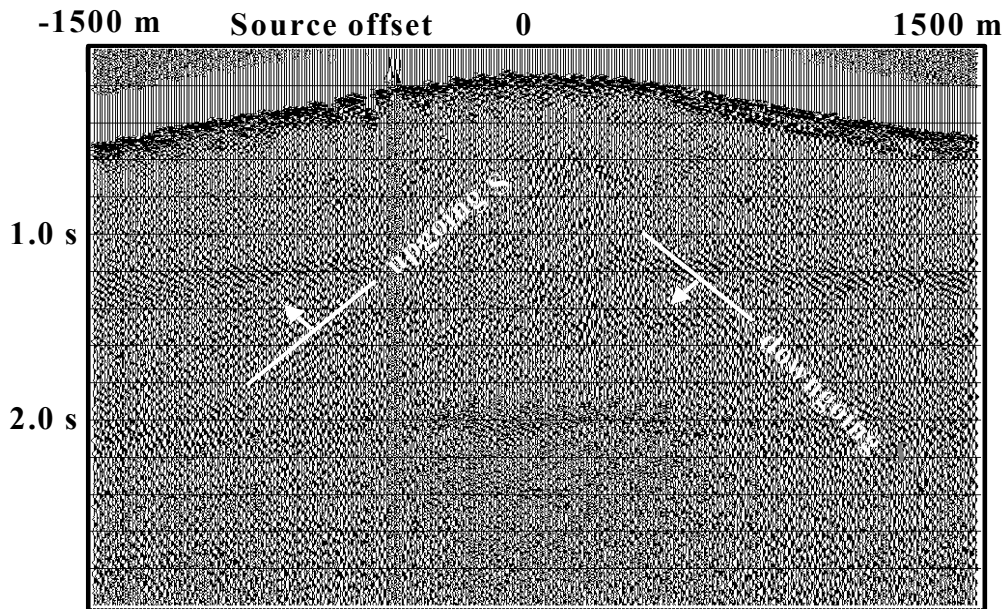
Blackfoot vsp supergather (raw inline horizontal wavefield)

Figure 4. Supergather formed from Blackfoot 3-C walk-away VSP inline horizontal component data sorted by source-borehole offset and receiver depth. Coherence direction for upgoing and downgoing S wave components indicated.

-1500 m   **Source offset**   **0**   **1500 m**
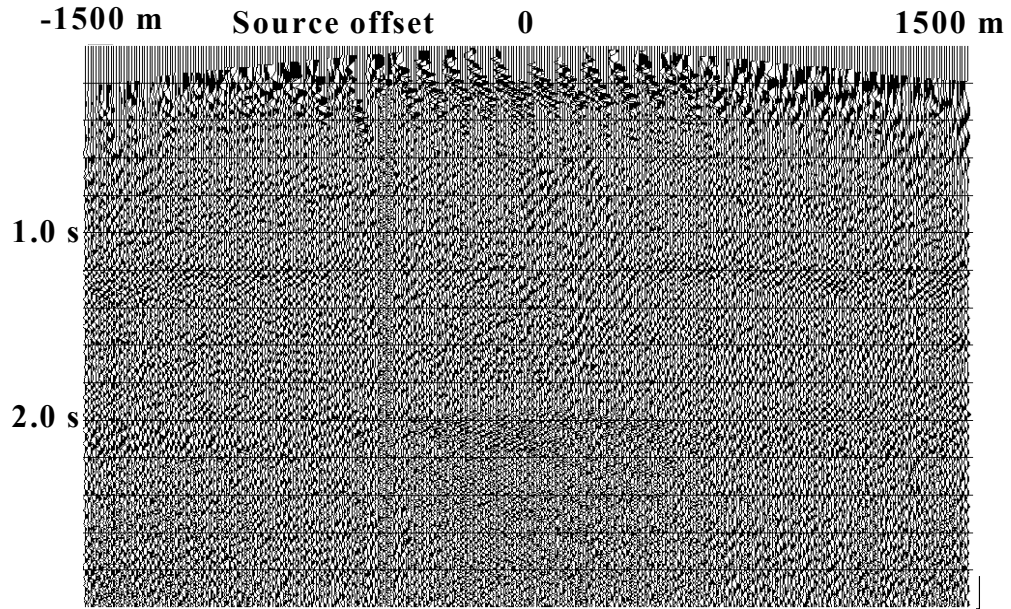
Blackfoot vsp supergather (flat inline horizontal component)

Figure 5. Inline supergather after NMO correction for source-borehole offset and linear moveout correction for receiver depth.

-1500 m   **Source offset**   **0**   **1500 m**
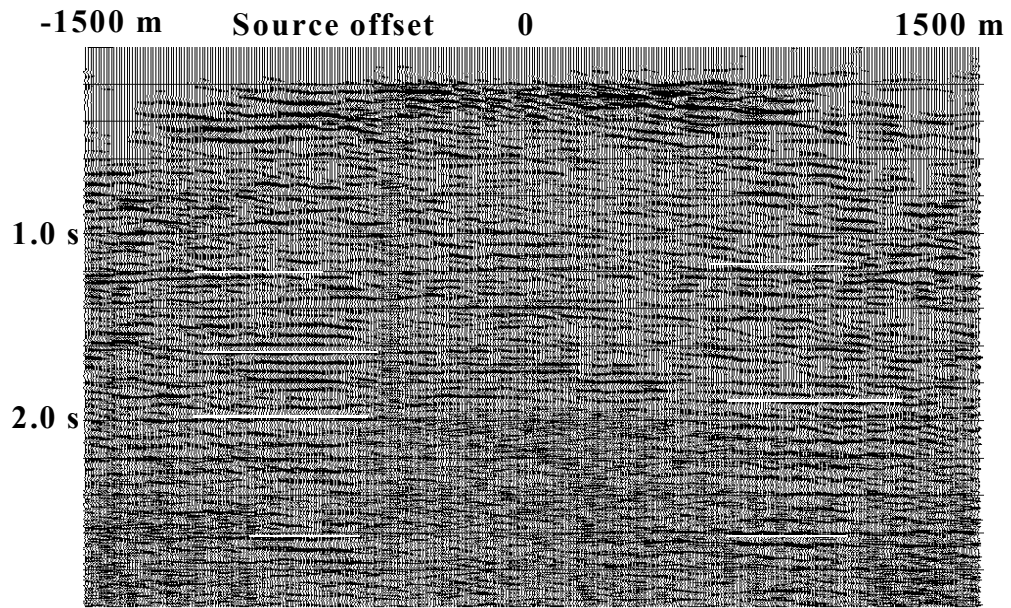
Blackfoot vsp supergather (upgoing inline wavefield)

Figure 6. Inline supergather after application of several passes of radial trace dip filtering to attenuate unwanted wavefield components and enhance upgoing inline wavefield.
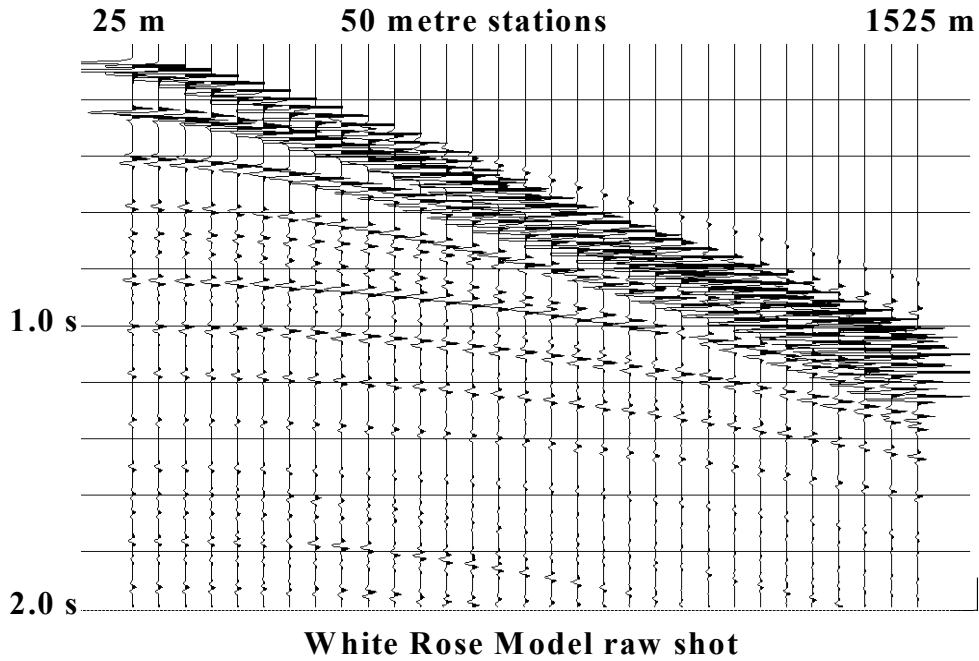
Figure 7. Synthetic marine shot gather generated to study OBC data. Many events on this gather are badly aliased.
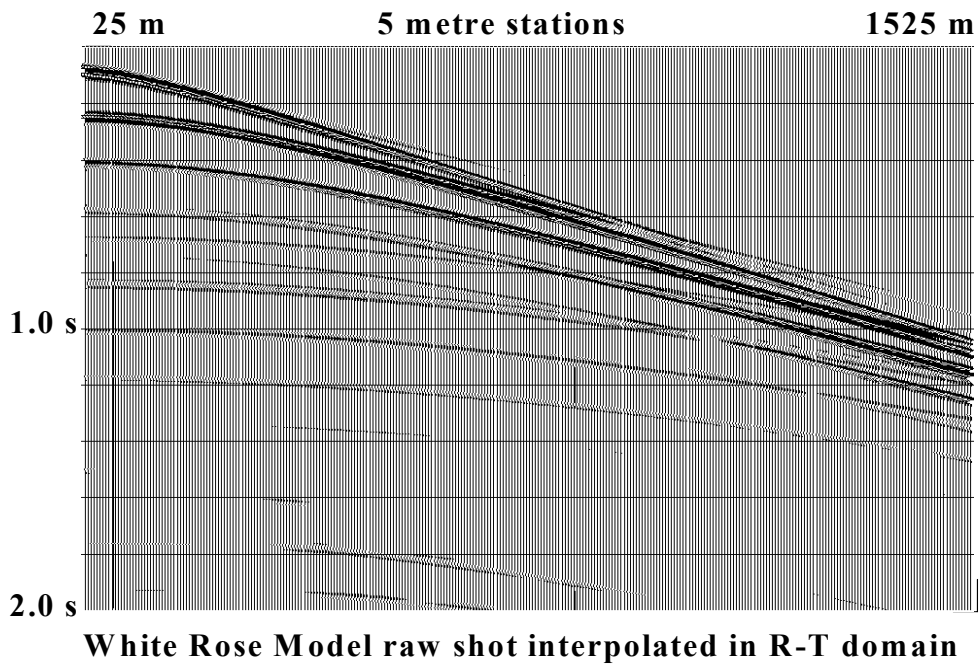

Figure 8. Synthetic shot gather after interpolation to finer station spacing in the radial trace transform. Spatial aliasing has been greatly reduced.
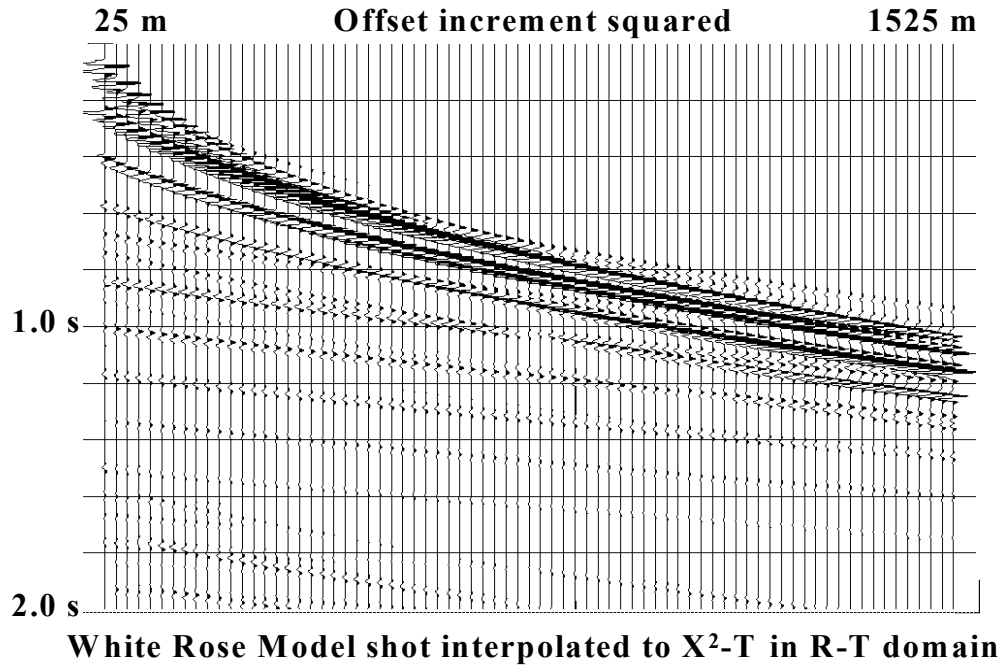
25 m **Offset increment squared** **1525 m**

1.0 s

2.0 s

White Rose Model shot interpolated to X²-T in R-T domain

Figure 9. Synthetic shot gather interpolated to squared offset increment in the radial trace transform.

25 m **Offset increment squared** **1525 m**

Sample increment squared

Hyperbolic portions of events are linear
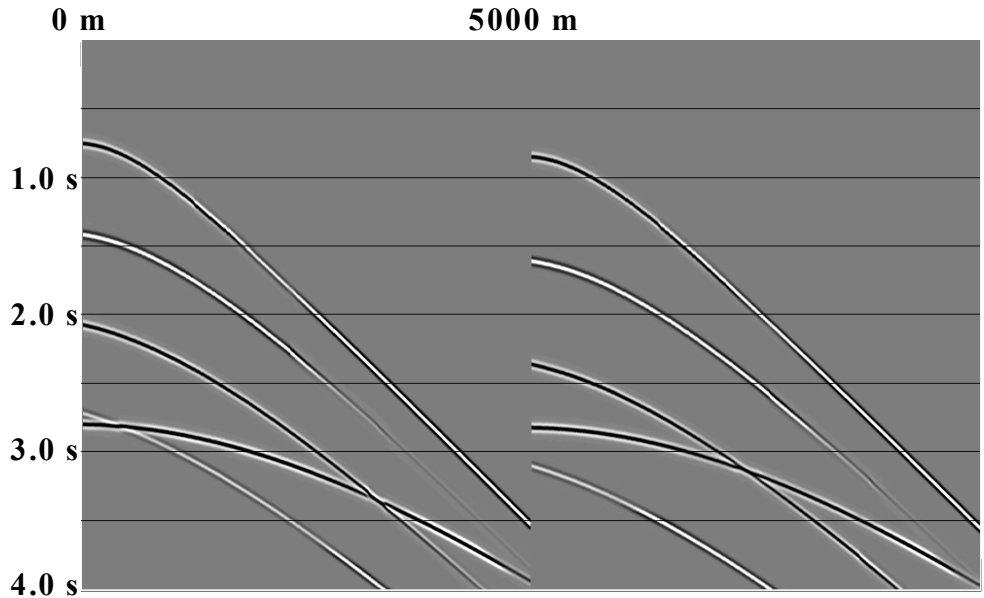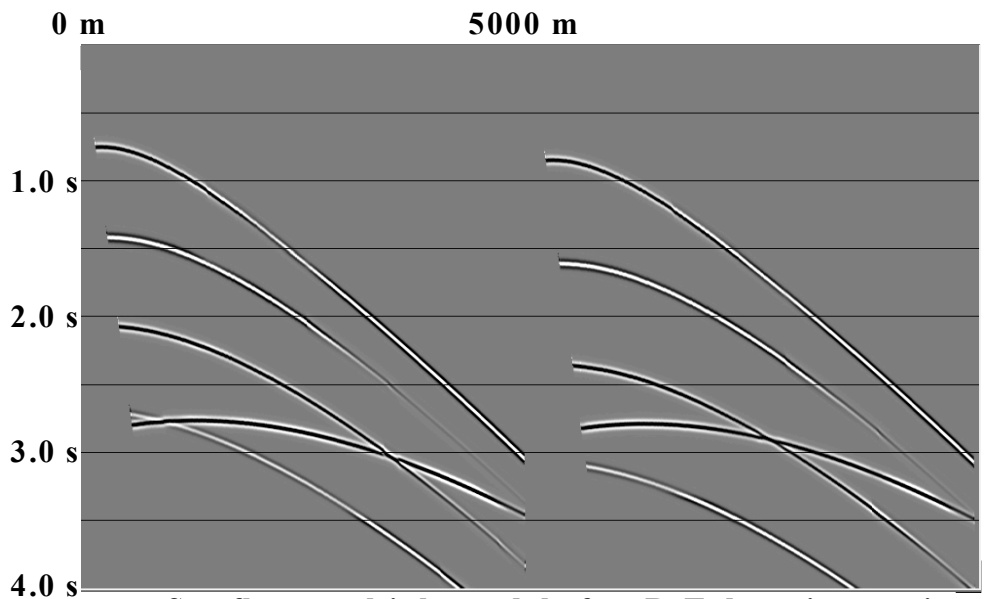
1.2 s

White Rose Model shot interpolated to X²-T² in R-T domain
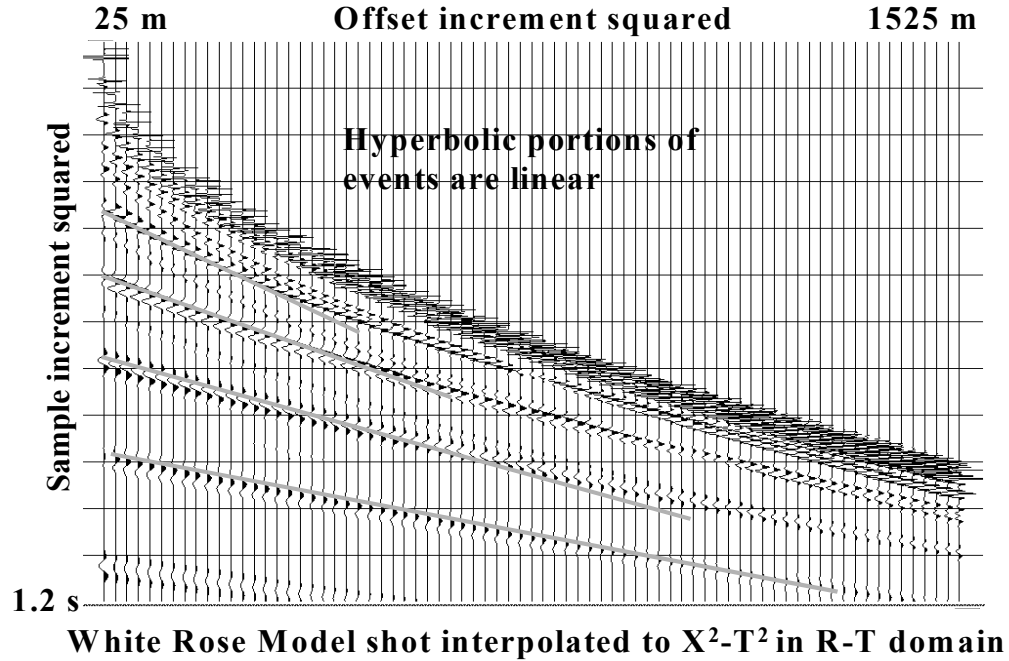
Figure 10. Synthetic shot gather interpolated to squared increments along both axes in the radial trace transform.

0 m   **5000 m**

Sea floor multiple model with 7.5 deg sea floor slope

Figure 11. Synthetic marine shot gathers generated by ray-tracing a simple model with sea-floor slope of 7.5 degrees.

0 m   **5000 m**

Sea floor multiple model after R-T domain rotation

Figure 12. Synthetic marine shot gather from 7.5 degree sloping sea floor after being rotated in the radial trace domain to simulate flat sea floor response.

0 m/sec   1500 m/sec

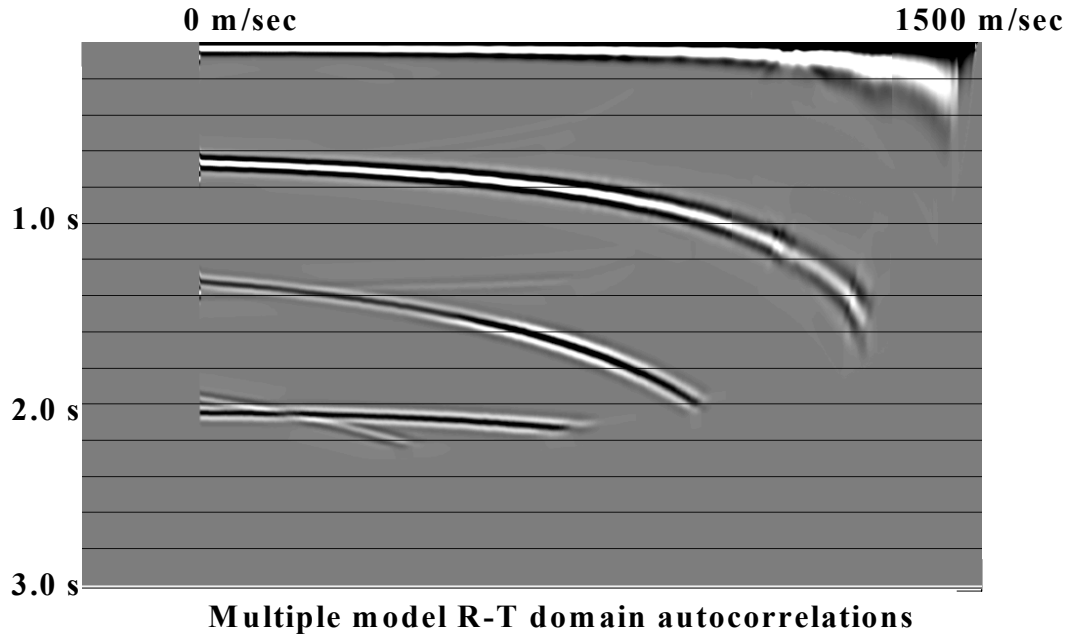**Multiple model R-T domain autocorrelations**

Figure 13. Autocorrelations of radial trace transform of the shot gather in Figure 11 (without radial trace domain rotation).

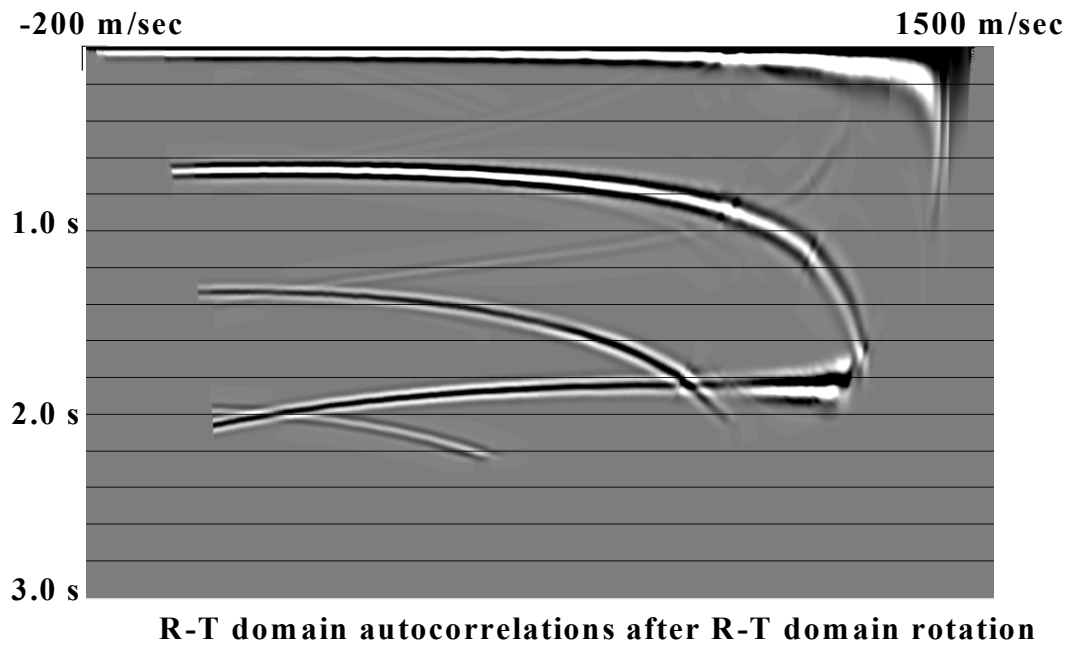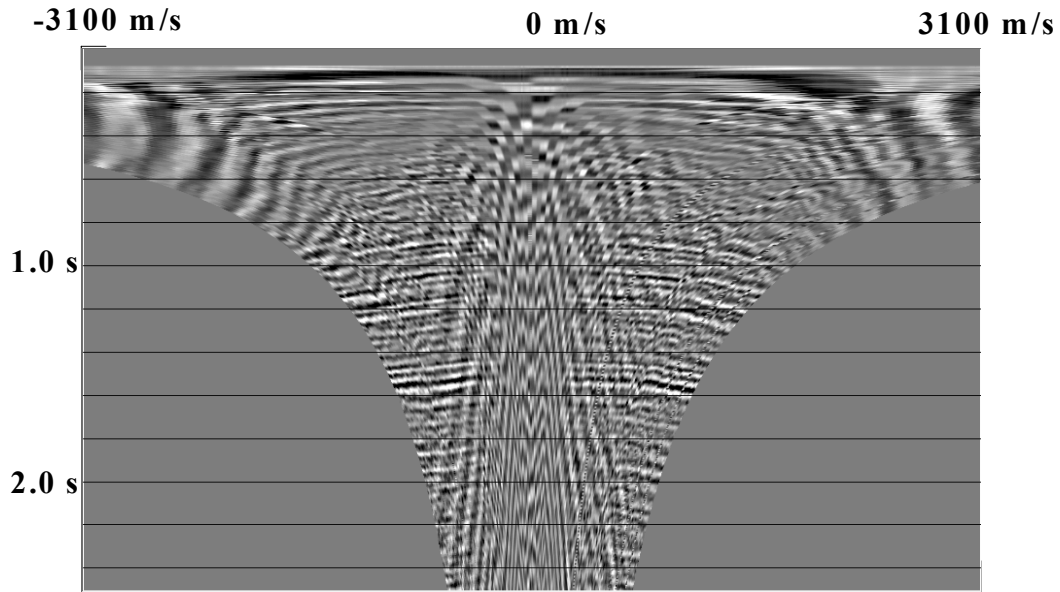-200 m/sec   1500 m/sec
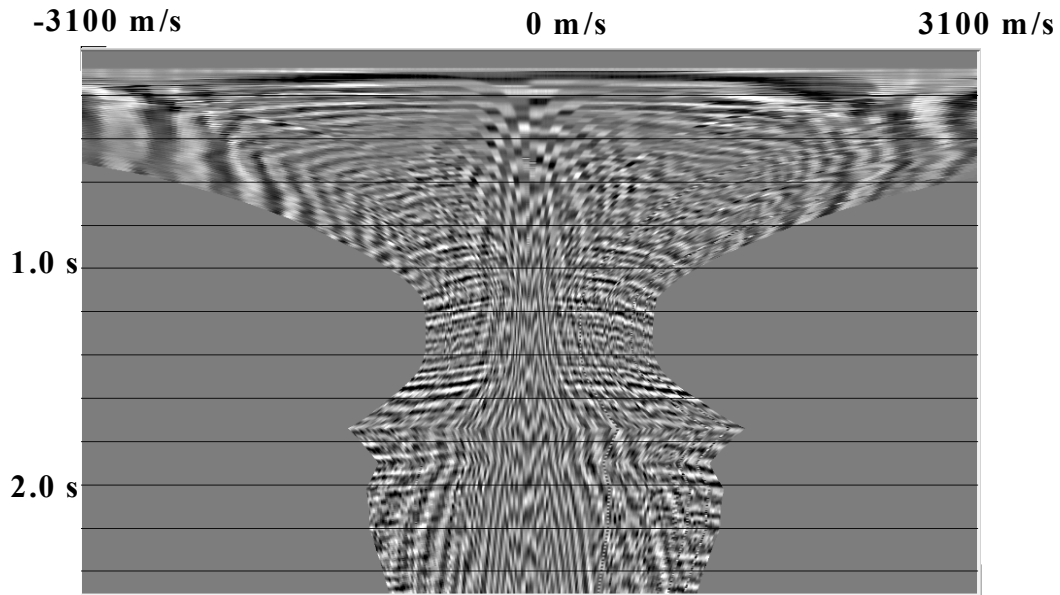

R-T domain autocorrelations after R-T domain rotation

Figure 14. Autocorrelations of radial trace transform of the shot gather in Figure 12 (after radial trace domain rotation).

-3100 m/s   **0 m/s**   **3100 m/s**

Conventional R-T transform

Figure 15. Standard radial trace transform of a Blackfoot shot gather.

-3100 m/s   **0 m/s**   **3100 m/s**

Snell Ray R-T transform

Figure 16. Snell ray radial trace transform of Blackfoot shot gather.